



Utilizing the Drake Passage Time-series to understand variability and change in subpolar Southern Ocean $p\text{CO}_2$

Amanda R. Fay¹, Nicole S. Lovenduski², Galen A. McKinley¹, David R. Munro², Colm Sweeney^{3,4}, Alison R. Gray⁵, Peter Landschützer⁶, Britton B. Stephens⁷, Taro Takahashi¹, and Nancy Williams⁸

¹Lamont Doherty Earth Observatory of Columbia University, New York, NY, USA

²Department of Atmospheric and Oceanic Sciences and Institute of Arctic and Alpine Research, University of Colorado, Boulder, CO, USA

³Cooperative Institutes for Research in Environmental Sciences, University of Colorado, Boulder, CO, USA

⁴NOAA Earth System Research Laboratory, Boulder, CO, USA

⁵School of Oceanography, University of Washington, Seattle, WA, USA

⁶Max Planck Institute for Meteorology, Hamburg, Germany

⁷National Center for Atmospheric Research (NCAR), Boulder, CO, USA

⁸College of Earth, Ocean, and Atmospheric Sciences, Oregon State University, Corvallis, OR, USA

Correspondence: Amanda R. Fay (afay@ldeo.columbia.edu)

Received: 15 November 2017 – Discussion started: 1 December 2017

Revised: 27 May 2018 – Accepted: 5 June 2018 – Published: 25 June 2018

Abstract. The Southern Ocean is highly under-sampled for the purpose of assessing total carbon uptake and its variability. Since this region dominates the mean global ocean sink for anthropogenic carbon, understanding temporal change is critical. Underway measurements of $p\text{CO}_2$ collected as part of the Drake Passage Time-series (DPT) program that began in 2002 inform our understanding of seasonally changing air–sea gradients in $p\text{CO}_2$, and by inference the carbon flux in this region. Here, we utilize available $p\text{CO}_2$ observations to evaluate how the seasonal cycle, interannual variability, and long-term trends in surface ocean $p\text{CO}_2$ in the Drake Passage region compare to that of the broader subpolar Southern Ocean. Our results indicate that the Drake Passage is representative of the broader region in both seasonality and long-term $p\text{CO}_2$ trends, as evident through the agreement of timing and amplitude of seasonal cycles as well as trend magnitudes both seasonally and annually. The high temporal density of sampling by the DPT is critical to constraining estimates of the seasonal cycle of surface $p\text{CO}_2$ in this region, as winter data remain sparse in areas outside of the Drake Passage. An increase in winter data would aid in reduction of uncertainty levels. On average over the period 2002–2016, data show that carbon uptake has strengthened with annual surface ocean $p\text{CO}_2$ trends in the Drake Passage and the

broader subpolar Southern Ocean less than the global atmospheric trend. Analysis of spatial correlation shows Drake Passage $p\text{CO}_2$ to be representative of $p\text{CO}_2$ and its variability up to several hundred kilometers away from the region. We also compare DPT data from 2016 and 2017 to contemporaneous $p\text{CO}_2$ estimates from autonomous biogeochemical floats deployed as part of the Southern Ocean Carbon and Climate Observations and Modeling project (SOCCOM) so as to highlight the opportunity for evaluating data collected on autonomous observational platforms. Though SOCCOM floats sparsely sample the Drake Passage region for 2016–2017 compared to the Drake Passage Time-series, their $p\text{CO}_2$ estimates fall within the range of underway observations given the uncertainty on the estimates. Going forward, continuation of the Drake Passage Time-series will reduce uncertainties in Southern Ocean carbon uptake seasonality, variability, and trends, and provide an invaluable independent dataset for post-deployment assessment of sensors on autonomous floats. Together, these datasets will vastly increase our ability to monitor change in the ocean carbon sink.

1 Introduction

The Southern Ocean plays a disproportionately large role in the global carbon cycle. Over the past few decades, the ocean has absorbed approximately 26 % of the carbon dioxide (CO₂) emissions from fossil fuel burning and land use change (Le Quéré et al., 2016, 2018), and since the preindustrial era, the ocean has been the primary sink for anthropogenic emissions (McKinley et al., 2017; Ciais et al., 2013). The Southern Ocean (south of 30° S) accounts for almost half of the total oceanic sink of anthropogenic CO₂ (Frölicher et al., 2015; Gruber et al., 2009; Takahashi et al., 2009). Though the importance of this region is widely understood, the relative scarcity of surface ocean carbon-related observations in the Southern Ocean hampers our ability to understand how this anthropogenic CO₂ uptake occurs against the background of natural variability.

Observations and models suggest large variability in the strength of Southern Ocean CO₂ uptake on decadal timescales. Several studies have reported a slow-down or reduction in the efficiency of Southern Ocean CO₂ uptake from the 1980s to the early 2000s (Le Quéré et al., 2007; Lovenduski et al., 2008, 2015; Metzl 2009; Takahashi et al., 2012; Fay and McKinley, 2013; Landschützer et al., 2014a, 2015a), followed by a substantial strengthening of the Southern Ocean CO₂ sink since 2002 (Fay and McKinley, 2013; Fay et al., 2014; Landschützer et al., 2015a; Munro et al., 2015a; Xue et al., 2015). Continued observational sampling efforts and coordination are required for quantifying and understanding decadal changes in this important CO₂ sink region.

Initiated in 2002 and continuing to the present, the Drake Passage Time-series is unique among Southern Ocean research programs in both its spatial and temporal coverage. High-frequency underway observations of the surface ocean partial pressure of CO₂ ($p\text{CO}_2$) are collected on Antarctic Research and Supply Vessel *Laurence M. Gould* on up to 20 crossings per year from the southern tip of South America to the Antarctic Peninsula, spanning the Antarctic Circumpolar Current (ACC) and its associated Antarctic Polar Front (Munro et al., 2015a, b). The DPT is also notable for sampling surface ocean $p\text{CO}_2$ during the austral winter in all years from 2002 to the present, providing valuable information about the full seasonal cycle of $p\text{CO}_2$ in the poorly sampled Southern Ocean. Other ships have contributed observations in the Drake Passage region, including the *Polarstern* and the *Nathaniel B. Palmer*; however, none has the consistent temporal coverage as provided by the DPT.

The surface ocean $p\text{CO}_2$ observations from the DPT have provided the foundation for larger datasets, which have been extensively used to examine variability and trends in CO₂ uptake in the broader Southern Ocean (Fay and McKinley, 2013; Fay et al., 2014; Majkut et al., 2014; Landschützer et al., 2014b, 2015b; Rödenbeck et al., 2015; Gregor et al., 2018). In many of these studies, interpolated estimates of

Southern Ocean $p\text{CO}_2$ are used in conjunction with measurements of atmospheric $p\text{CO}_2$ to estimate variability and trends in the air–sea $p\text{CO}_2$ gradient and, when combined with wind speed, air–sea CO₂ fluxes.

The physical oceanography of the Drake Passage region is unique in the Southern Ocean. Here, the strong flow of the zonally unbounded ACC is funneled through a narrow constriction (~ 800 km), making it an ideal location for sampling across the entire ACC system over a relatively short distance (Sprintall et al., 2012). At the same time, the unique nature of this circulation could potentially reduce the degree to which the Drake Passage region is representative of the broader subpolar region. The DPT program takes advantage of frequent *Gould* crossings to conduct physical and biogeochemical sampling of the ACC system. Thus, before conclusions can be drawn about large-scale Southern Ocean carbon uptake and its variability using data from the DPT, it is important to document how $p\text{CO}_2$ in this particular region compares with $p\text{CO}_2$ measured elsewhere in the subpolar Southern Ocean. In this study, we utilize available ship-based surface ocean $p\text{CO}_2$ observations collected in the subpolar Southern Ocean to evaluate how the seasonal cycle, interannual variability, and long-term trends of surface ocean $p\text{CO}_2$ in the Drake Passage region compare to that of the broader subpolar Southern Ocean. Further, we highlight the opportunity for post-deployment assessment of autonomous observational platforms passing through the Drake Passage utilizing the high-frequency, underway $p\text{CO}_2$ measurements from the DPT.

2 Data

This study uses several observational datasets and data products of surface ocean $p\text{CO}_2$ in the Southern Ocean: measurements from the Surface Ocean CO₂ Atlas (SOCAT), which includes underway measurements from the DPT, interpolated estimates of the SOCAT data using a self-organizing map feed-forward neural network (SOM-FFN) approach, and calculated $p\text{CO}_2$ estimates from biogeochemical Argo floats. While the SOCAT database reports the fugacity of carbon dioxide ($f\text{CO}_2$), for our analysis we consider datasets reporting $p\text{CO}_2$ and $f\text{CO}_2$ to be interchangeable. This is an acceptable assumption for surface ocean observations as CO₂ behaves closely to an ideal gas. Globally, the difference between these parameters is less than 2 μatm , with $f\text{CO}_2$ being smaller than $p\text{CO}_2$ by no more than 2 μatm due to temperature dependence. This is roughly the reported uncertainty of shipboard observations of $p\text{CO}_2$ and well within the uncertainty of the observation-based $p\text{CO}_2$ estimates. Below, we describe each of these data sources in turn.

2.1 The Drake Passage Time-series (DPT)

A unique dataset of ongoing year-round observations beginning in 2002 is available from the Drake Passage Time-series. This dataset provides an unprecedented opportunity to characterize the mean and time-varying state of the Drake Passage and surrounding waters using direct observations. In addition to high-frequency underway observations of surface ocean $p\text{CO}_2$, other physical and biogeochemical variables measured onboard allow for a complete understanding of the carbonate system in the Drake Passage. Analytical methods used to measure $p\text{CO}_2$ to $\pm 2 \mu\text{atm}$ are described in detail by Munro et al. (2015a, b).

2.2 Surface Ocean CO_2 Atlas (SOCAT)

SOCAT is a global surface ocean carbon dataset of $f\text{CO}_2$ values ($p\text{CO}_2$ corrected for the non-ideal behavior of CO_2) (Sabine et al., 2013; Pfeil et al., 2013). In this study, we utilize version 5 of this product (SOCATv5) and include data with a reported WOCE flag of 2 and cruise flags A–D, which results in a dataset of roughly 18.5 million observations globally, spanning years 1957–2016, with uncertainties of ± 2 – $5 \mu\text{atm}$ (Bakker et al., 2016). This dataset includes over 740 000 observations contributed from the DPT. Despite the large number of observations available in the Southern Ocean, data are spatially and temporally concentrated, with strong seasonal biases. Most data are collected during reoccupations of supply routes to Antarctic bases or on repeat hydrographic lines, which leaves large bands of the Southern Ocean completely unsampled (Bakker et al., 2016).

2.3 Self-Organizing Map Feed-forward Network Product (SOM-FFN)

Landschützer et al. (2014b) use a two-step neural network approach to extrapolate the monthly gridded SOCAT product in space and time. This results in reconstructed, basin-wide monthly maps of the sea surface $p\text{CO}_2$ at a resolution of $1^\circ \times 1^\circ$ (Landschützer et al., 2017). Air–sea CO_2 flux maps are then computed using a standard gas exchange parameterization and high-resolution wind speeds. The neural network estimate is described and substantially validated in past publications (Landschützer et al., 2014a, 2015a, 2016) and it was shown that the estimates fit observed $p\text{CO}_2$ data in the Southern Ocean with a root mean square error (RMSE) of about $20 \mu\text{atm}$ and with almost no bias (Landschützer et al., 2015a, Supplement).

The SOM-FFN product used in this analysis was created from SOCATv5. Additionally, we generated an alternative SOM-FFN product (SOM-FFN-noDP) using the same methodological setup but excluding the $p\text{CO}_2$ data collected in the Drake Passage region for years 2002–2016, which represents the years of the DPT program.

2.4 SOCCOM floats

The Southern Ocean Carbon and Climate Observations and Modeling (SOCCOM) project (<http://soccom.princeton.edu>, last access: 2 April 2018) aims to deploy approximately 200 biogeochemical profiling floats over a 5-year period (2015 to 2020) in an effort to fill observational gaps in the Southern Ocean. In total, over 100 floats carrying some combination of additional biogeochemical sensors (i.e., pH, nitrate, oxygen, fluorescence, and backscattering) have been collecting data since April 2014 (Johnson et al., 2017). With the float's capability to measure pH and utilization of existing algorithms for predicting total alkalinity, $p\text{CO}_2$ can be calculated from the collected observations and compared to underway observations (Williams et al., 2017).

The uncertainty range for these calculated $p\text{CO}_2$ values is estimated to be 2.7% ($\pm 11 \mu\text{atm}$ at $400 \mu\text{atm}$) and takes into account multiple sources of uncertainty, including measurement error, uncertainties introduced through the quality control procedures, and uncertainties in seawater carbonate system thermodynamics (Williams et al., 2017). $p\text{CO}_2$ estimates from profiling floats have not been included in the SOCAT database because they do not directly measure surface water CO_2 . For consistency, we maintain this separation in our analysis and limit our study of SOCCOM floats to direct comparisons to DPT values in Sect. 5.

3 Methods

The SOCATv5 database from 2002 to 2016 is considered here to match the years of overlap with DPT observations, which began in 2002. The SOCAT dataset is then subsampled to include only observations with reported salinity values in the 33.5–34.5 range and a distance-to-land value greater than or equal to 50 km. This step restricts our analysis to open-ocean observations, since coastal observations report lower salinity values, which correspond to low $p\text{CO}_2$ values due to the influence of freshwater and ice melt. SOCCOM float files were downloaded on 2 April 2018 and reported $p\text{CO}_2$ values are an average of all data collected in the top 20 m of water, calculated using alkalinity derived from the LIAR algorithm (Carter et al., 2016), to remain consistent with previous SOCCOM float analysis.

The Southern Ocean region of interest is the Southern Ocean Subpolar Seasonally Stratified (SPSS) biome as defined in Fay and McKinley (2014) as the region of the Southern Hemisphere with climatological SST $< 8^\circ\text{C}$ but excluding areas with a sea-ice fraction greater than or equal to 50% (Fig. 1). While the SPSS biome encompasses the Drake Passage, we further define a Drake Passage region as the portion of the Southern Ocean SPSS biome bounded by 55 and 70° W lines of longitude (Fig. 1, black box). This is similar to the region analyzed in Munro et al. (2015a); however, it

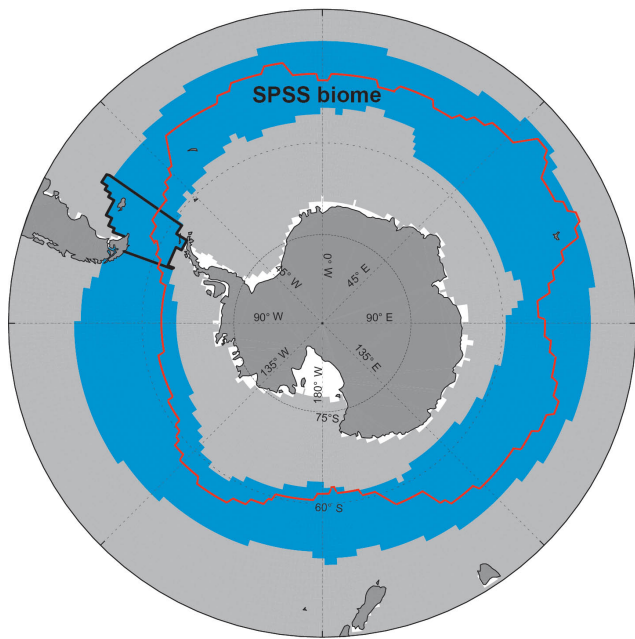


Figure 1. Map of the Subpolar Seasonally Stratified (SPSS) biome (Fay and McKinley, 2014), defined at $1^\circ \times 1^\circ$ resolution. The red line represents the mean location of the Antarctic Polar Front (Freeman and Lovenduski, 2016), interpolated to a $1^\circ \times 1^\circ$ grid. The black box represents the Drake Passage region considered in this analysis.

extends the region of interest to the northern and southern extents of the SPSS biome.

In order to compare the seasonal cycle and long-term trends in the Drake Passage with the broader SPSS biome, we analyze surface ocean $p\text{CO}_2$ from three subsets of the SOCAT database: SOCAT-all, which includes all available SOCATv5 data from 2002 to 2016 in the SPSS biome, SOCAT-DP, which includes SOCATv5 data within the longitudinally defined Drake Passage region (Fig. 1, with 62 % of these data obtained by the LDEO/Univ. Colorado group), and SOCAT-noDP, which excludes any data within the longitudinally defined Drake Passage region of the SPSS biome. All datasets are first averaged to monthly, $1^\circ \times 1^\circ$ resolution. Monthly means are then calculated for the SPSS biome by first removing the background mean annual climatological value of $p\text{CO}_2$ at each $1^\circ \times 1^\circ$ location (Landschützer et al., 2014a) to aid in accounting for the potential of spatial aliasing in the sparsely sampled Southern Ocean (Fay and McKinley, 2013).

Alternate definitions of the larger Southern Ocean region of interest were considered during our analysis, including a subdivision of the SPSS into a Northern SPSS and Southern SPSS, with the boundary defined by the location of the mean position in the Antarctic Polar Front (Freeman and Lovenduski, 2016; Freeman et al., 2016; Munro et al., 2015b). As discussed in Munro et al. (2015a), Drake Passage Time-series observations north of the front report higher $p\text{CO}_2$ values

than to the south, and they find a larger trend in $p\text{CO}_2$ in the north for years 2002–2015. Additionally, the seasonal cycle amplitude north of the front is much larger and well defined than south of the front. We see these patterns in the SOCAT dataset as well; however, given the goal of this research, we choose to consider the entire north-to-south extent of the SPSS as a whole. Outside of the Drake Passage region, available data are limited such that analysis over northern and southern subregions would be impossible.

Additionally, we consider analysis over the Polar Antarctic Zone (PAZ), defined as the area between the Subantarctic Front and the sea-ice zone (Williams et al., 2017) (Supplement Fig. S1). While differences exist in trends and seasonality when using the PAZ definition (Supplement Figs. S2–3), the overall conclusions of the relationship between SOCAT-DP and SOCAT-all remain largely unchanged when using this alternate regional definition.

Biome-scale monthly means are compared and used to calculate seasonal cycles and trends. Seasonal cycles are calculated by first removing a $1.95 \mu\text{atm yr}^{-1}$ trend to account for increasing atmospheric CO_2 during the 2002–2015 period (Dlugokencky et al., 2015). Seasonal uncertainties (Fig. 2) are estimated as 1 standard error from the mean of all available biome mean values for a given month. This is a conservative estimate of the uncertainty in any given month because of inconsistent annual coverage and spatial undersampling biases. Reported trends are calculated by fitting a single harmonic and linear trend to the biome-scale monthly means as done in Fay and McKinley (2013). Trends are not statistically different if the calculated mean seasonal cycle is removed instead of the choice to fit a harmonic to the data. Seasonal trends are calculated with a simple linear fit to the seasonal monthly means.

4 Results and discussion

4.1 Seasonal cycle

The mean seasonal cycle of $p\text{CO}_2$ (corrected to reference year 2002) in the Southern Ocean SPSS biome for the three SOCAT datasets and the full SOM-FFN estimate indicates broad agreement (Fig. 2). Here, surface ocean $p\text{CO}_2$ levels reach a maximum in austral winter (June to August), when deep mixing delivers carbon-rich water to the surface, and a minimum in austral summer (December to February), when biological production draws down the inorganic carbon from the surface (Takahashi et al., 2009). Temperature also plays a role in modulating the $p\text{CO}_2$ seasonal cycle in the Southern Ocean. Winter cooling drives $p\text{CO}_2$ lower at the same time as deep winter mixing elevates surface carbon levels. During the summer, warming temperatures raise $p\text{CO}_2$, while biological utilization of carbon drives surface $p\text{CO}_2$ levels lower (Munro et al., 2015b).

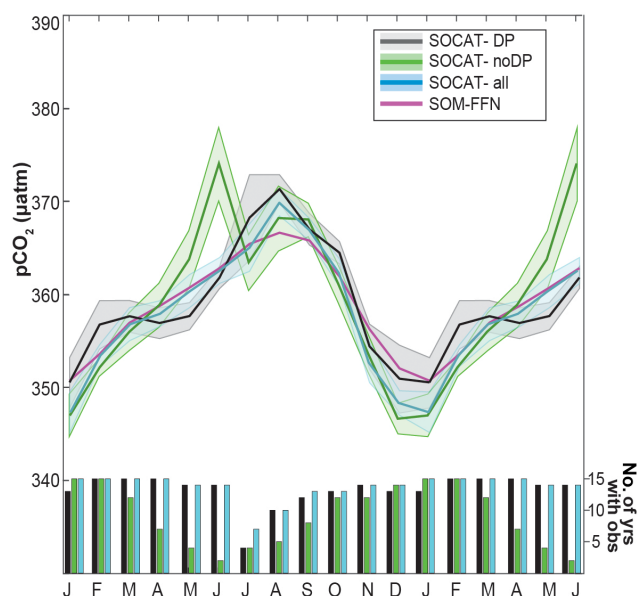


Figure 2. Mean surface ocean $p\text{CO}_2$ seasonal cycle estimate for years 2002–2016, for the SPSS biome from each dataset, shown on an 18-month cycle, calculated from a time series corrected to year 2002 (atmospheric trend of $1.95 \mu\text{atm yr}^{-1}$ removed). Shading represents 1 standard error for biome-scale monthly means driven by interannual variability; there is no error represented for SOM-FFN. Bar plot indicates the number of years containing observations in a given month (maximum of 15 years) for the SOCAT-DP, SOCAT-noDP, and SOCAT-all datasets.

The average amplitude of the detrended seasonal cycle of $p\text{CO}_2$ (max–min) is $23 \mu\text{atm}$ (Fig. 2), smaller than the high-latitude oceans in the Northern Hemisphere (Takahashi et al., 2002, 2009; Landschützer et al., 2015b). The small amplitude of the $p\text{CO}_2$ seasonal cycle in this region is due to the similar magnitude and opposite phasing of temperature and carbon supply/utilization effects (Munro et al., 2015b). In all months, mean surface ocean $p\text{CO}_2$ levels in the Southern Ocean SPSS are below atmospheric, which ranges from a global annual mean of 372 ppmv in 2002 to 399 ppmv in 2015, indicating that this region has been a persistent CO_2 sink over the period of analysis (Dlugokencky and Tans, 2017).

Figure 2 also shows the uncertainty of the seasonal mean, with shading representing 1 standard error from the monthly mean for each dataset, defined as the standard deviation divided by the square root of the sample size (here, number of years with available data in that month). Uncertainty estimates vary for each month of the seasonal cycle, with a minimum uncertainty of $1.1 \mu\text{atm}$ (June, SOCAT-DP) to a maximum of $5 \mu\text{atm}$ (July, SOCAT-DP). These estimates are of the same magnitude as the measurement accuracy of underway $p\text{CO}_2$ in SOCAT ($\pm 2\text{--}5 \mu\text{atm}$).

Figure 3 indicates how diverse Southern Ocean $p\text{CO}_2$ data density is in space and time. Compared to the regular sam-

pling of the DPT, there are many fewer repeated occupations of SR03 south of Australia (Shadwick et al., 2015), along the Prime Meridian (Hoppema et al., 2009; Van Heuven et al., 2011), and in the southwestern Indian sector (Metzl et al., 1999; Lo Monaco et al., 2005, 2010; Metzl, 2009). Specifically, during austral winter, data availability outside of the Drake Passage region is extremely limited due to the few ships operating in winter and the difficult conditions that the wintertime Southern Ocean presents to data collection efforts (Fig. 3b).

Despite irregular sampling, average seasonal cycles of the three SOCAT datasets are quite similar, with few statistically significant differences given the uncertainty bounds. SOCAT data from the Drake Passage region (SOCAT-DP, gray) exhibit relatively large estimated uncertainty (average for all months = $2.22 \mu\text{atm}$), despite the frequent coverage and smaller region considered. This indicates that large interannual variability is inherent to the Drake Passage region, especially in the well-observed austral summer months. Despite data being much more regularly collected in this region than in the rest of the Southern Ocean (Fig. 3), there are still months of quite limited observations, specifically July and August (Fig. 2). SOCAT-all has monthly uncertainties averaging $1.7 \mu\text{atm}$, with the largest uncertainties in January and July (Fig. 2, blue). Data availability for SOCAT-all is consistent for much of the year, with most months having observations in at least 13 of the 15 years considered in this analysis (Fig. 2). The exceptions are July and August, which have data from only 8 and 10 years, respectively.

The SOCAT-noDP seasonal cycle is similar to that of the other datasets, but deviates in the austral fall/winter, specifically May and June. In winter, SOCAT-noDP suggests higher $p\text{CO}_2$ than SOCAT-DP or SOCAT-all, though the limited data in June and July must be considered when drawing conclusions from this difference (Figs. 2, 3b). With June and July data available for fewer than 5 of the 15 years covered in the analysis it is possible that the peak shown here could be biased by the few years included, specifically for the month of June. In contrast, SOCAT-DP has data for nearly all of the years considered in these months. The data that are available during May and June in SOCAT-noDP are from regions downstream of the Drake Passage (Fig. 3b).

Seasonal cycles are consistent when analyzing the PAZ region (Supplement Fig. S2); however, the SOCAT-DP seasonal cycle exhibits two maxima, possibly due to the omission of the southern area of the Drake Passage (Supplement Fig. S1), which would cause values for the PAZ region to be greater than those shown for the DP region of the SPSS. The June peak in SOCAT-noDP also remains when considering the PAZ region. Amplitudes are comparable given the uncertainty; however, the seasonal amplitude for each dataset is slightly larger over the SPSS biome than the PAZ, likely due to the more northern expansion of the PAZ region downstream of the Drake Passage and the exclusion of the southern Drake Passage region in the boundary of the PAZ.

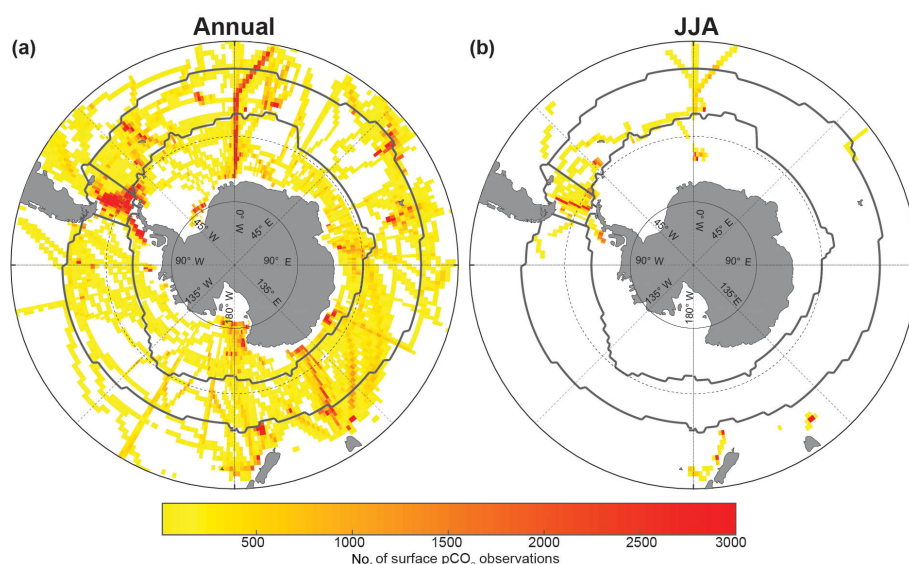


Figure 3. Data density of $p\text{CO}_2$ observations from the SOCATv5 dataset within each $1^\circ \times 1^\circ$ grid cell. Data are restricted to years 2002–2016. Salinity values outside of 33.5–34.5 psu and observations within 50 km of land are omitted. (a) Data from all months of the year; (b) data from only June, July, and August (austral winter). Gray lines designate the boundary of the SPSS biome and the Drake Passage region for reference.

Overall, given available data, the seasonal cycles are statistically indistinguishable for data collected inside and outside of the Drake Passage region, for all months with at least 5 years of observations (Fig. 2). This analysis of SOCAT $p\text{CO}_2$ data indicates that the Drake Passage seasonal cycle is representative of the broader SPSS biome seasonality, based on the available observations to date, but increased observations outside of the Drake Passage during May and June are needed to provide a more robust comparison. Additionally, the seasonal cycles from all three SOCAT datasets closely resemble the smoothed seasonality of the interpolated SOM-FFN product in the SPSS biome (Fig. 2). Sparse sampling outside of the Drake Passage during winter months leads to this estimated seasonal cycle of SOCAT-all being driven by Drake Passage data. Enhanced wintertime data collection, especially in regions outside of the Drake Passage, is required to better constrain the full seasonal cycle of surface ocean $p\text{CO}_2$ in the Southern Ocean SPSS.

4.2 Interannual variability

The high resolution of the time-series data in the Drake Passage allows for close examination of temporal variability in $p\text{CO}_2$ with relatively low uncertainty (Munro et al., 2015a). We investigate the interannual variability in Drake Passage $p\text{CO}_2$ in Fig. 4a, where deseasonalized and detrended anomalies (Fay and McKinley, 2013) from the SOCAT-DP dataset are shown in gray, with the black line representing these anomalies smoothed with a 12-month running mean. Over the 2002–2016 period, the variance in $p\text{CO}_2$ anomalies is $66 \mu\text{atm}^2$. Monthly anomalies are as large as $\pm 30 \mu\text{atm}$,

and 12-month smoothed anomalies as large as $\pm 12 \mu\text{atm}$ in this dataset.

A model-based study by Lovenduski et al. (2015) finds interannual variability in $p\text{CO}_2$ to be low in the Drake Passage compared to other Southern Ocean regions for years 1981–2007. In contrast, we find that detrended and deseasonalized anomalies from SOCAT-noDP and SOCAT-DP have comparable variances (59 and $66 \mu\text{atm}^2$). This result, however, is likely strongly affected by the previously discussed seasonal data gaps outside of the DP region or potentially by the different years considered in these two analyses. Conducting a similar analysis of the reported SOCAT sea surface temperature (SST) values does find the variance for SOCAT-DP to be significantly lower than SOCAT-noDP (0.93 and $2.72 \text{ }^\circ\text{C}^2$, respectively). As the same sampling issues exist for SST as for $p\text{CO}_2$ in SOCAT, an alternate method to address this issue is needed to resolve these conflicting results.

The SOM-FFN data product offers complete seasonal and regional coverage, and thus the comparison of variance in the Drake Passage to all of the Southern Ocean can be made in this context. Results for SOM-FFN are different from both the SOCAT findings above and the results of Lovenduski et al. (2015). For the SPSS biome area of SOM-FFN $p\text{CO}_2$, the variance of detrended and deseasonalized anomalies is significantly higher within the Drake Passage region than outside of the region (14.2 and $6.2 \mu\text{atm}^2$, respectively). It should be noted that variances are significantly lower for the SOM-FFN because of its interpolation. We are left without a clear picture as to whether the Drake Passage is more or less variable in $p\text{CO}_2$ than the rest of the Southern Ocean SPSS. This conundrum is clearly due to the lack of data availability,

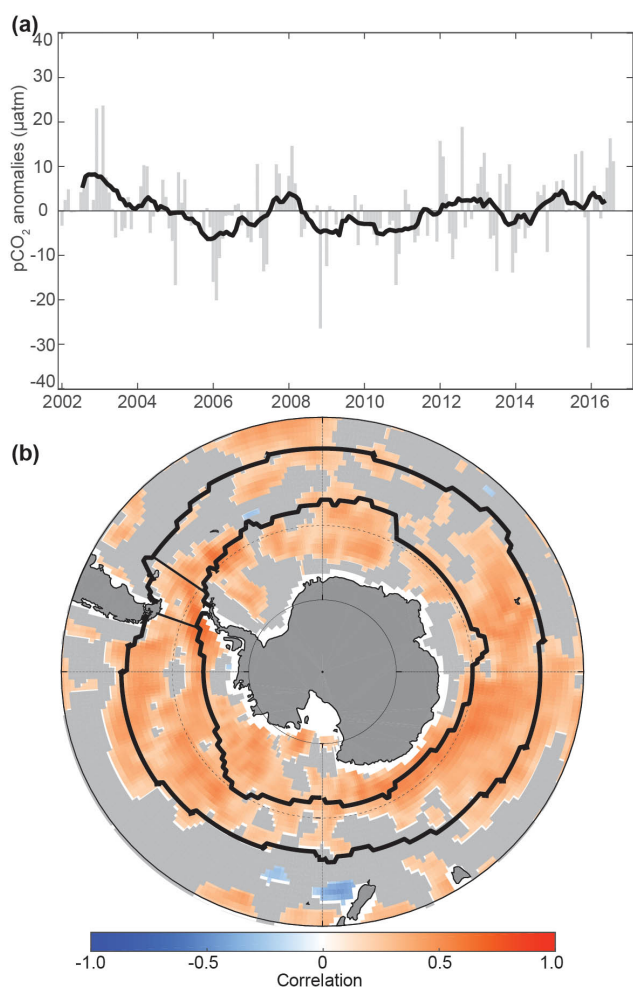


Figure 4. (a) Temporal evolution of deseasonalized, detrended monthly SOCAT-DP $p\text{CO}_2$ anomalies (gray bars) over 2002–2016, with 12-month running averages (black line) overlain. (b) Correlation between monthly SOCAT-DP $p\text{CO}_2$ anomalies and the $p\text{CO}_2$ anomalies estimated from the SOM-FFN-noDP product (created without the inclusion of Drake Passage data), for years 2002–2016 at each $1^\circ \times 1^\circ$ grid cell. Gray shading represents areas where the correlation does not pass significance t -tests at $p < 0.05$.

particularly outside the Drake Passage during winter months (Fig. 3b).

Given the lack of data, the degree to which the Drake Passage represents interannual variability within the Southern Ocean SPSS can only be considered in the context of the SOM-FFN data product. To produce independent estimates of correlations between the Drake Passage and other points, we use a version of the SOM-FFN product created without the inclusion of any observations in our defined Drake Passage region (SOM-FFN-noDP, Fig. 4b), and assess correlations with SOCAT data within the Drake Passage. Anomalies have been detrended and deseasonalized, and grayed areas indicate that the correlation is not significant at the 95 % confidence level (Fig. 4b). The strongest positive correlations

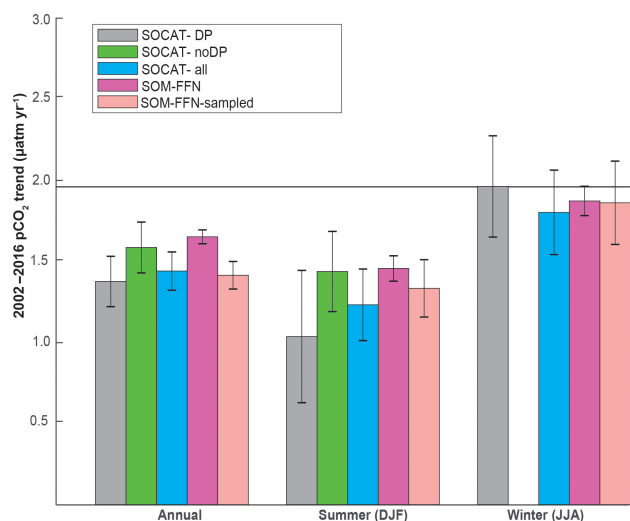


Figure 5. Surface ocean $p\text{CO}_2$ trends in the SPSS biome for years 2002–2016 ($\mu\text{atm yr}^{-1}$): SOCATv5 data within the Drake Passage box (gray); SOCATv5 data excluding data from the Drake Passage box (green); SOCATv5 (blue); SOM-FFN product (magenta); SOM-FFN $p\text{CO}_2$ product sampled as SOCATv5 data in the Drake Passage box (light pink). The figure includes annual trends (left), austral summer trends (center) and austral winter trends (right). SOCAT-noDP winter trend omitted because it did not contain a JJA value for every year of the time series. For reference, the atmospheric $p\text{CO}_2$ trend during the 2002–2015 period ($1.95 \mu\text{atm yr}^{-1}$) is shown as a horizontal black line.

are within the Drake Passage, upstream of the Drake Passage into the central Pacific SPSS, and in the Indian Ocean sector of the SPSS biome (Fig. 4b). Weaker positive correlations are found in the western Pacific SPSS, as well as a few areas in the Atlantic sector of the SPSS. No regions of widespread strong negative correlations are observed in the SPSS biome. This is consistent with the analysis of Munro et al. (2015b), who estimate the footprint of the Drake Passage extending upstream into the eastern Pacific sector of the ACC.

4.3 Trends, 2002–2016

Trends for all data (annual), as well as summer (DJF) and winter (JJA), are estimated from the three SOCAT datasets, the SOM-FFN data product, and the SOM-FFN product subsampled as SOCAT-DP (SOM-FFN-sampled), in all cases following the approach of Fay and McKinley (2013). Similar to the climatological $p\text{CO}_2$ seasonal cycle, annual trends for the three SOCAT datasets are indistinguishable given the 68 % confidence intervals (Fig. 5, Supplement Table S1).

All annual trends are less than the 2002–2016 atmospheric $p\text{CO}_2$ trend of $1.95 \mu\text{atm yr}^{-1}$ (Dlugokencky et al., 2015), indicating that the Southern Ocean has been a growing sink for atmospheric carbon over 2002–2016 (Fig. 5, far left). Comparing the different estimates, SOCAT-DP (gray bar) and SOCAT-all (blue bar) have annual trends slightly below

that of the full SOM-FFN, however with greater uncertainty bounds. The annual trend from the SOCAT-all dataset (blue) is nearly identical to the SOCAT-DP trend in both mean and uncertainty. These are not statistically different from the SOCAT-noDP, although the SOCAT-noDP dataset does yield a slightly larger annual trend. While SOCAT-noDP yields the largest annual trend of the three datasets, it still falls well below the atmospheric trend. These trends are comparable to those reported in Munro et al. (2015b), Takahashi et al. (2012), and Fay et al. (2014), despite these studies utilizing different datasets, methods, and regional boundaries. Takahashi et al. (2014), similar to Munro et al. (2015b), show that trends in the northern portion of the Drake Passage are greater than those south of the front. Our analysis of regions north and south of the front confirms this (not shown).

Sampling the SOM-FFN data product as the SOCAT-DP dataset (SOM-FFN-sampled) is one way to estimate the impact of the available data coverage in the Drake Passage region as compared to the hypothetical situation of perfect data coverage in the SPSS biome. Sampling lowers the trend, making it significantly smaller than the full SOM-FFN trend. This reduction leads to an annual trend very similar to that of SOCAT-DP and SOCAT-all. This conclusion emphasizes the need for increased observations around the Southern Ocean as it implies we are potentially not accurately capturing the true trend in this region with the available data coverage.

Conclusions of these comparisons are largely maintained for summer and winter trends (Fig. 5, center and right). Uncertainty increases when considering seasonal trends due to reduced data quantity. All trends are statistically indistinguishable for summer months; however, the SOCAT-DP trend shows the largest change from the reported annual trends. For winter, SOCAT-noDP is not shown, because unlike SOCAT-all and SOCAT-DP, not all years have available data during this season (Fig. 2). Overall, winter trends are slightly higher than summer trends. Even given the uncertainties, winter and summer trends are clearly distinguishable for SOCAT-DP, SOCAT-all, and the full and sampled SOM-FFN product. In each of these datasets, the winter trend is roughly $0.5 \mu\text{atm yr}^{-1}$ higher than the summer trend. While winter trends have larger differences and larger uncertainties, consistent with reduced data availability, this seasonal difference in trends is significant. Further and more detailed consideration of this seasonal comparison is warranted. Initial investigations indicate that 2016 had anomalously high wintertime $p\text{CO}_2$ values (not shown). Specifically, when trends are calculated with the same datasets for 2002–2015, winter trends are significantly lower than the atmospheric trend (SOCAT-DP: $1.53 \pm 0.32 \mu\text{atm yr}^{-1}$, SOCAT-all: $1.59 \pm 0.27 \mu\text{atm yr}^{-1}$, SOM-FFN: $1.70 \pm 0.09 \mu\text{atm yr}^{-1}$). It is important to consider the impact of anomalous values at the end of selected time series, specifically for time series less than 15 years (Fay and McKinley, 2013).

An investigation of trends from the full SOM-FFN product and that of the SOM-FFN-noDP product for the entire

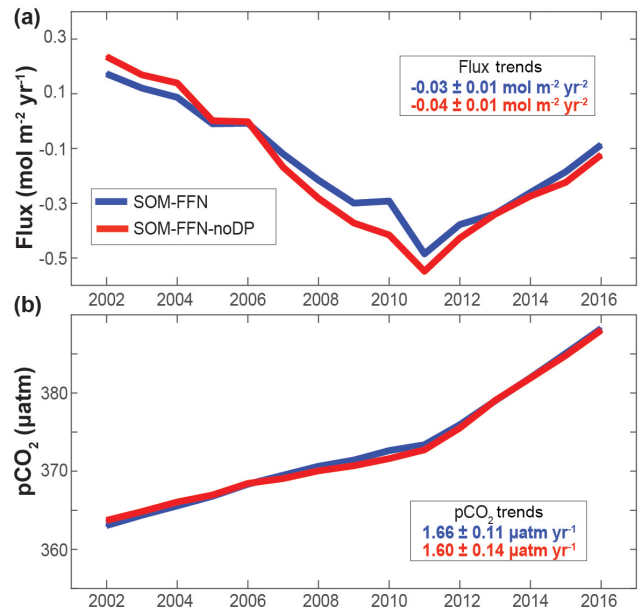


Figure 6. (a) Sea–air CO_2 flux and (b) $p\text{CO}_2$ averaged over the Southern Ocean SPSS biome, from the SOM-FFN $p\text{CO}_2$ product (blue) and that of the SOM-FFN-noDP product created without the inclusion of Drake Passage data (red). Trends and uncertainty values in corresponding colors.

Southern Ocean SPSS biome for years 2002–2016 indicates an increasing carbon uptake by the ocean with some interannual variability (Fig. 6). If the Drake Passage data are omitted during the creation of the product (SOM-FFN-noDP), carbon flux and $p\text{CO}_2$ trends are unchanged (Fig. 6). Both estimates illustrate that for 2002–2016, the Southern Ocean SPSS biome was an important sink of carbon dioxide.

Trend analysis for the PAZ region (Supplement Fig. S3, Supplement Table S1) produces comparable results. Annual trends are indistinguishable between the three SOCAT datasets as well as between the SOM-FFN product, both full and sampled. It could be that the greater extent of the PAZ northward yields better agreement between the datasets and the SOM-FFN product. All annual trends are also below the atmospheric trend. Summer and winter trends for the PAZ are consistent with results for the SPSS biome, with winter trends being larger than summer trends, most significantly for the SOCAT-DP and SOM-FFN datasets. While actual trend values are different from those shown in Fig. 2, the results show that the relationship between trends for the three SOCAT datasets are indistinguishable for both seasons and annual analyses.

5 DPT as a $p\text{CO}_2$ evaluation point for biogeochemical profiling floats

Starting in late 2014, autonomous biogeochemical profiling floats have been deployed as part of the SOCCOM project,

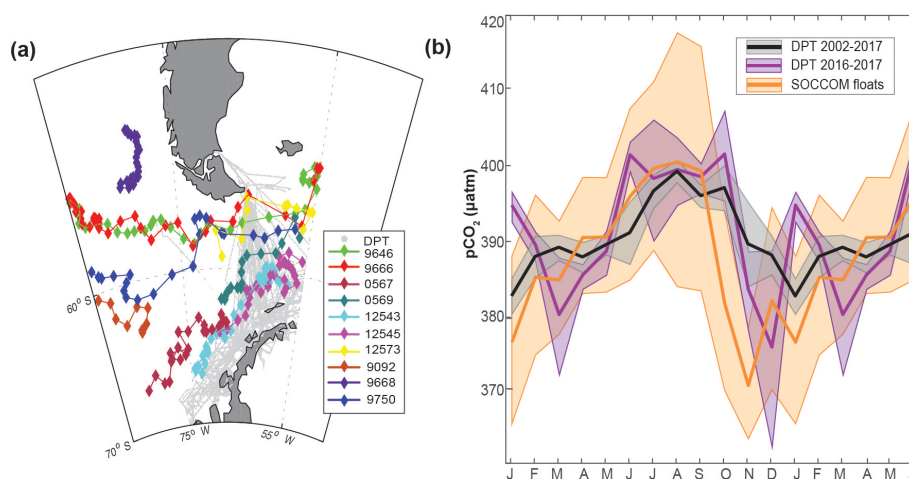


Figure 7. (a) Trajectories of Drake Passage-transiting SOCCOM floats included in this analysis. Colored diamonds represent the locations of surface measurements for each float. Data from floats collected east of 55° W and west of 90° W are not included in this analysis. Gray dots represent observations from the DPT. (b) Mean surface ocean $p\text{CO}_2$ seasonal cycle estimate for black: underway Drake Passage Time-series data for years 2002–2016; purple: DPT for years 2016–2017 to match years covered by the floats; and orange: SOCCOM floats. Seasonal cycles are shown on an 18-month cycle, calculated from a monthly mean time series with the atmospheric correction to year 2017. Shading represents 1 standard error accounting for the spatial and temporal heterogeneity of the sample and the measurement error (2.7 % or $\pm 11 \mu\text{atm}$ at a $p\text{CO}_2$ of $400 \mu\text{atm}$ for floats; $\pm 2 \mu\text{atm}$ for DPT data) combined using the square root of the sum of squares.

and as of December 2017, 10 floats had traveled through or were approaching the Drake Passage region (Fig. 7a). These floats offer a new opportunity to complement our oceanographic understanding that has been developed primarily with traditional shipboard observations. Results above show that a lack of observations outside of the Drake Passage region may contribute to the large uncertainties in both seasonality and trends, which limits the conclusions we are able to make with currently available shipboard data. As floats provide autonomous, near-real-time observations covering existing spatial and temporal gaps throughout the Southern Ocean and ship-based systems provide high density observations at higher accuracy ($\pm 2.7\%$ or $11 \mu\text{atm}$ at a $p\text{CO}_2$ of $400 \mu\text{atm}$ for floats compared to $\pm 2 \mu\text{atm}$ for ships), there is great potential for these two platforms to work in concert to provide a whole Southern Ocean carbon observing system. However, there are limitations of float observations, notably the indirect estimate of $p\text{CO}_2$ from pH and the requirement to adjust the sensor calibrations post-deployment by reference to deep (near 1500 m) pH values estimated from multiple linear regression equations fitted to high-quality, spectrophotometric pH observations made on repeat hydrography cruises (Williams et al., 2016, 2017; Johnson et al., 2016, 2017). Further comparisons between float-estimated $p\text{CO}_2$ and shipboard observations are clearly warranted, and the complementary strengths of the Drake Passage Time-series make it an ideal dataset to help address these issues.

Here we utilize the underway Drake Passage Time-series $p\text{CO}_2$ data to conduct comparisons to nearby SOCCOM floats, considering both seasonality as well as fine-scale crossovers. Note that in this section of the analysis we utilize

data only from the Drake Passage Time-series (Takahashi et al., 2017, available at <https://www.nodc.noaa.gov/ocads/data/0160492.xml>) instead of the SOCATv5 dataset because SOCAT data are not available after 2016 at the time of writing.

A strong benefit of autonomous observation systems is their ability to sample regions and times that are not often surveyed by ships. SOCCOM floats collect data throughout the year, and especially important are the additional observations in austral winter, a time when there are limited opportunities for ship-based measurements. While currently only 2 full years of data are available from floats within the Drake Passage (2016–2017), they span the full width of the region (Fig. 7a) and are able to observe during each month of the year. A seasonal comparison of monthly mean $p\text{CO}_2$ values for the DPT data and float $p\text{CO}_2$ estimates within the defined Drake Passage region show that both platforms capture the expected seasonal cycle for the subpolar Southern Ocean with a wintertime peak and summertime low (Fig. 7b). All datasets shown have been adjusted to 2017 using the mean atmospheric trend ($1.95 \mu\text{atm yr}^{-1}$) (Dlugokencky et al., 2015), and thus mean values are higher than shown in the seasonal curves of Fig. 2. Standard error shading on the seasonal cycles (Fig. 7b) includes considerations of measurement accuracy as this differs substantially between these two platforms. Shading represents 1 standard error accounting for the spatial and temporal heterogeneity of the sample and measurement error (2.7 % or $\pm 11 \mu\text{atm}$ at a $p\text{CO}_2$ of $400 \mu\text{atm}$ for floats; $\pm 2 \mu\text{atm}$ for DPT data), combined using the square root of the sum of squares.

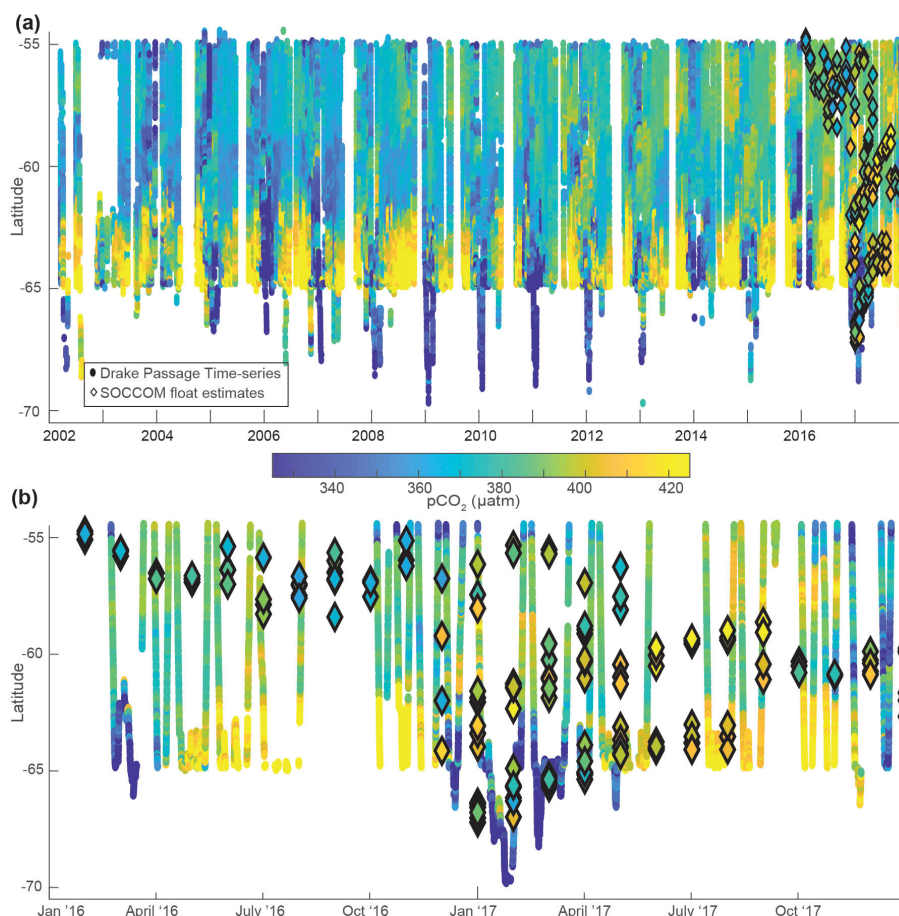


Figure 8. (a) 2002–2017 underway DPT $p\text{CO}_2$ observations (circles) and surface $p\text{CO}_2$ estimates from SOCCOM floats overlain (diamonds; μatm), plotted versus latitude. (b) Same as (a) but plotted as January 2016 to December 2017.

The seasonal cycle derived from float-estimated $p\text{CO}_2$ has a larger seasonal amplitude compared to the DPT data from 2002 to 2017, due to an earlier and much lower observed summertime minimum. The difference in summertime minima is smaller however when DPT data from only 2016 and 2017 are considered (Fig. 7b). The remaining difference between the floats and the DPT 2016–2017 data might be an artifact of the specific locations sampled, as floats and ships are not exactly synchronous, as well as the conditions specific to 2016 and 2017. In summer 2016 for example, the floats appear to have captured a strong phytoplankton bloom to the north and upstream of the Drake Passage, not captured by the DPT, that resulted in strong inorganic carbon uptake and low $p\text{CO}_2$; the floats did not sample in the southern region where $p\text{CO}_2$ is substantially higher in the early spring (Fig. 8). However, there is no indication from the 2002–2017 seasonal cycle that this low excursion of the $p\text{CO}_2$ persists when looking at the entire Drake Passage region (Fig. 7b). Since phytoplankton blooms typically progress southward during spring (Carranza and Gille, 2015) this difference in

phasing likely results from the floats sampling preferentially the earlier northern uptake.

Underway Drake Passage Time-series $p\text{CO}_2$ data in the SPSS biome have a large range, often spanning over $100 \mu\text{atm}$ each month as shown in the time series in Fig. 8, largely related to the 10°C temperature gradient and associated physical and biological dynamics that are captured over the region. $p\text{CO}_2$ from all floats east of 90° and west of 55° W is also plotted on the time series (Fig. 8, diamonds), with the reported $p\text{CO}_2$ value being an average for all depths shallower than 20 m. Float-based $p\text{CO}_2$ surface estimates largely fall within the range of the direct underway $p\text{CO}_2$ observations; however, notable differences do exist when spatial and temporal differences are taken into consideration. Float estimates from the central Drake Passage in winter (JJA) 2017 (Fig. 8b) are higher than nearby DPT observations, though cruise data do not precisely overlap in time. Overall, the range of the DPT observations is far larger than the range of estimated $p\text{CO}_2$ from floats inside the Drake Passage region because they regularly span across the full width of the Drake Passage where meridional decorrelation length scales

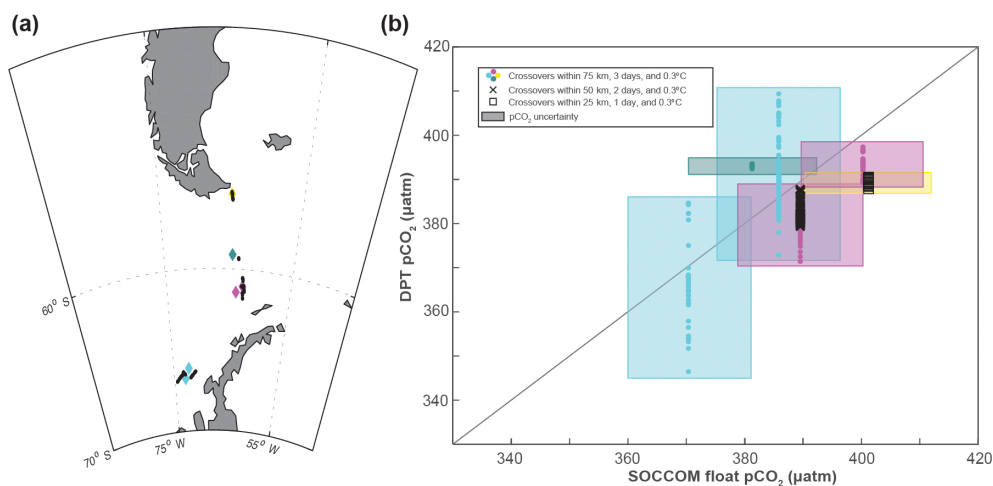


Figure 9. (a) Map of SOCCOM floats with DPT crossovers within 75 km, 3 days, and 0.3 °C SST from coincident surface observations. (b) Calculated $p\text{CO}_2$ from the SOCCOM float (x -axis) versus DPT underway $p\text{CO}_2$ observations (y -axis) for crossover float locations, with a 1 : 1 line. Colors correspond to the float number in Fig. 7. Horizontal width of shading represents SOCCOM relative standard uncertainty, which is estimated at $\pm 2.7\%$ μatm ; vertical shading is $\pm 2\ \mu\text{atm}$. Black “x” and squares indicated crossovers within a smaller window (50 km/2 day/0.3 °C SST and 25 km/1 day/0.3 °C SST, respectively).

are relatively short (Eveleth et al., 2017). Conversely, floats tend to sample along the path of the ACC.

As floats offer autonomous, frequent observations and ships offer data of the highest quality, it is ideal for these two platforms to work in partnership. Analysis of direct comparisons between DPT data and SOCCOM floats at crossover points indicates more precisely this potential (Fig. 9). As of December 2017, there have been six occurrences of floats surfacing near DPT observations within a window of 75 km, 3 days, and have a reported SST within 0.3 °C of each other (Fig. 9a). This window is consistent with the crossover criteria used by the SOCAT community to quality control shipboard data (Pfeil et al., 2013; Olsen et al., 2013). Figure 9a shows locations of the floats and the nearby DPT observations that fit this crossover window. As DPT offers high-frequency observations, all available measurements over the 3-day window are shown (Fig. 9b). Also indicated are DPT observations that cross over within a 50 km and 2-day window and 25 km and 1-day window (Fig. 9b, black “x” and squares, respectively), both also with the 0.3 °C SST criteria.

This comparison of the calculated $p\text{CO}_2$ from the floats and observed DPT $p\text{CO}_2$ reveals a broad correspondence (passing through the 1 : 1 line) in all six crossover instances within the $\pm 2.7\%$ relative standard uncertainty of the SOCCOM float measurements and $\pm 2\ \mu\text{atm}$ DPT uncertainty (Fig. 9b shading). While all float crossovers do intersect the 1 : 1 line given their stated uncertainties, these comparisons reveal the large range of $p\text{CO}_2$ captured by high-frequency shipboard measurements in a relatively small region and illustrate that this range cannot be fully captured by floats surfacing only once every 10 days. Further investigation of crossovers in the entire Southern Ocean region is needed; the

DPT provides the most likely occurrence for this, although other regions with frequent ship traffic and autonomous platforms with biogeochemical capabilities should also be utilized when feasible. Additional post-deployment data quality checks using the underway surface $p\text{CO}_2$ data from DPT and other ship-based programs should be conducted, and more thorough assessments could be achieved if hydrocast observations were planned to occur in the vicinity of a passing biogeochemical float. Such coordinated efforts would significantly advance monitoring of the carbon cycle in the Southern Ocean.

6 Conclusions

The Drake Passage Time-series illustrates the large variability of surface ocean $p\text{CO}_2$ and exemplifies the value of sustained observations for understanding changing ocean carbon uptake in the Southern Ocean. This is the only location where carbon measurements throughout the entire annual cycle in the subpolar Southern Ocean have been made regularly over the past 2 decades. The available observations to date indicate that the Drake Passage seasonal cycle is representative of the seasonality observed for the entire SPSS biome, but increased observations outside of the Drake Passage, specifically during austral winter, are needed to provide a more robust comparison. Uncertainties in the seasonality for all datasets studied remain considerable given the dynamic nature of this region and the short time series considered. Specifically, a lack of winter data in all years limits the direct conclusions for differences between the Drake Passage and the larger SPSS biome where we see a discrepancy in the timing of the winter maxima. These findings can di-

rect specific goals for focus regions of future observations. Specifically, insufficient wintertime data in regions outside of the Drake Passage limit our assessment of how representative Drake Passage data are of the larger subpolar region.

The magnitude of interannual variability is comparable for SOCAT $p\text{CO}_2$ data within and outside of the Drake Passage region of the SPSS biome, a finding that conflicts with results from previous modeling and analysis of the SOM-FFN product. A clear idea of whether the Drake Passage is more or less variable in $p\text{CO}_2$ will require increased data, particularly during the austral winter, outside of the Drake Passage. Given these data restrictions, the representativeness of the larger SPSS biome is also investigated using the SOM-FFN product. Within this gap-filled data product, monthly anomalies in the Drake Passage region are representative of broad swaths of the Southern Ocean, specifically regions upstream of the Drake Passage, but strong relationships are also evident in regions in the Indian Ocean sector of the Southern Ocean. Consistent with this finding, estimates of long-term trends do not change substantially if observations in the Drake Passage are removed from the SOM-FFN analysis. Across approaches to data analysis, trends in annual oceanic $p\text{CO}_2$ trends for 2002–2016 are less than the atmospheric $p\text{CO}_2$ trend, confirming previous findings that the Southern Ocean has, on average, been a growing sink for atmospheric carbon over this period.

Comparisons between underway DPT measurements and SOCCOM float estimates taken within the Drake Passage show broad agreement, while a fine-scale crossover investigation demonstrates their direct correspondence given uncertainty ranges for SOCCOM float $p\text{CO}_2$ estimates. Continuation of high-temporal measurements of the DPT, in addition to expanded programs to target floats with both underway observations and frequent hydrocasts serving as independent datasets for post-deployment, will provide high-value comparisons, improving community confidence in float-based $p\text{CO}_2$ estimates. Coordinated monitoring efforts that combine a well-calibrated array of autonomous biogeochemical floats with a robust ship-based observational network will improve and expand monitoring of the carbon cycle in the Southern Ocean in the future.

Data availability. All data used in this study are publicly available. SOCAT data are available via <https://www.nodc.noaa.gov/archive/arc0108/0163180/2.2/data/0-data/SOCATv5.tsv> (last access: 2 April 2018). Drake Passage data are available via <https://www.nodc.noaa.gov/ocads/data/0160492.xml> ([https://doi.org/10.3334/CDIAC/OTG.NDP088\(V2015\)](https://doi.org/10.3334/CDIAC/OTG.NDP088(V2015)), Takahashi et al., 2017). SOCCOM float data are available via <https://library.ucsd.edu/dc/object/bb3450604r> (<https://doi.org/10.6075/J0PG1PX7>, Johnson et al., 2018).

The Supplement related to this article is available online at <https://doi.org/10.5194/bg-15-3841-2018-supplement>.

Competing interests. The authors declare that they have no conflict of interest.

Acknowledgements. We are grateful for funding from the NSF (PLR-1543457, OCE-1558225, OCE-1155240), the NOAA (NA12OAR4310058), and NASA (NNX17AK19G). NCAR is sponsored by the National Science Foundation. We acknowledge support from the Space Science and Engineering Center of University of Wisconsin – Madison and Columbia University. The authors are especially grateful for the efforts of the marine and science support teams of the ARSV *Laurence M. Gould*, particularly Timothy Newberger, Kevin Pedigo, Bruce Felix, and Andy Nunn. Underway DPT measurements presented in this paper are archived at the NOAA's National Centers for Environmental Information (https://www.nodc.noaa.gov/ocads/oceans/VOS_Program/LM_gould.html, last access: 2 April 2018). The Surface Ocean CO₂ Atlas (SOCAT) is an international effort, supported by the International Ocean Carbon Coordination Project (IOCCP), the Surface Ocean Lower Atmosphere Study (SOLAS), and the Integrated Marine Biogeochemistry and Ecosystem Research program (IMBER) to deliver a uniformly quality-controlled surface ocean CO₂ database. The many researchers and funding agencies responsible for the collection of data and quality control are thanked for their contributions to SOCAT. Float data were collected and made freely available by the Southern Ocean Carbon and Climate Observations and Modeling (SOCCOM) Project funded by the National Science Foundation, Division of Polar Programs (NSF PLR-1425989), supplemented by NASA, and by the International Argo Program and the NOAA programs that contribute to it (<http://www.argo.ucsd.edu>, <http://argo.jcommops.org>, last access: 2 April 2018). The Argo Program is part of the Global Ocean Observing System.

Edited by: Jack Middelburg

Reviewed by: two anonymous referees

References

- Bakker, D. C. E., Pfeil, B., Landa, C. S., Metzl, N., O'Brien, K. M., Olsen, A., Smith, K., Cosca, C., Harasawa, S., Jones, S. D., Nakaoka, S.-I., Nojiri, Y., Schuster, U., Steinhoff, T., Sweeney, C., Takahashi, T., Tilbrook, B., Wada, C., Wanninkhof, R., Alin, S. R., Balestrini, C. F., Barbero, L., Bates, N. R., Bianchi, A. A., Bonou, F., Boutin, J., Bozec, Y., Burger, E. F., Cai, W.-J., Castle, R. D., Chen, L., Chierici, M., Currie, K., Evans, W., Featherstone, C., Feely, R. A., Fransson, A., Goyet, C., Greenwood, N., Gregor, L., Hankin, S., Hardman-Mountford, N. J., Harlay, J., Hauck, J., Hoppema, M., Humphreys, M. P., Hunt, C. W., Huss, B., Ibáñez, J. S. P., Johannessen, T., Keeling, R., Kitidis, V., Körtzinger, A., Kozyr, A., Krasakopoulou, E., Kuwata, A., Landschützer, P., Lauvset, S. K., Lefèvre, N., Lo Monaco, C., Manke, A., Mathis, J. T., Merlivat, L., Millero, F. J., Monteiro, P. M. S., Munro, D. R., Murata, A., Newberger, T., Omar, A. M., Ono, T., Paterson, K., Pearce, D., Pierrot, D., Robbins, L. L., Saito, S., Salisbury, J., Schlitzer, R., Schneider, B., Schweitzer, R., Sieger, R., Skjelvan, I., Sullivan, K. F., Sutherland, S. C., Sutton, A. J., Tadokoro, K., Telszewski, M., Tuma, M., van Heuven, S. M. A.

- C., Vandemark, D., Ward, B., Watson, A. J., and Xu, S.: A multi-decade record of high-quality $f\text{CO}_2$ data in version 3 of the Surface Ocean CO_2 Atlas (SOCAT), *Earth Syst. Sci. Data*, 8, 383–413, <https://doi.org/10.5194/essd-8-383-2016>, 2016.
- Carranza, M. M. and Gille S. T.: Southern Ocean wind-driven entrainment enhances satellite chlorophyll-a through the summer, *J. Geophys. Res.-Oceans*, 120, 304–323, <https://doi.org/10.1002/2014JC010203>, 2015.
- Carter, B. R., Williams, N. L., Gray, A. R., and Feely, R. A.: Locally interpolated alkalinity regression for global alkalinity estimation, *Limnol. Oceanogr.-Meth.*, 14, 268–277, 2016.
- Ciais, P., Sabine, C., Bala, G., Bopp, L., Brovkin, V., Canadell, J., Chhabra, A., DeFries, R., Galloway, J., Heimann, M., Jones, C., Le Quéré, C., Myneni, R. B., Piao, S., and Thornton, P.: Carbon and Other Biogeochemical Cycles, in: *Climate Change 2013: The Physical Science Basis. Contribution of Working Group I to the Fifth Assessment Report of the Intergovernmental Panel on Climate Change*, edited by: Stocker, T. F., Qin, D., Plattner, G.-K., Tignor, M., Allen, S. K., Boschung, J., Nauels, A., Xia, Y., Bex, V., and Midgley, P. M., Cambridge University Press, Cambridge, United Kingdom and New York, NY, USA, 2013.
- Dlugokencky, E. and Tans, P.: NOAA/ESRL, www.esrl.noaa.gov/gmd/ccgg/trends/, last access: 15 September 2017.
- Dlugokencky, E. J., Masarie, K. A., Lang, P. M., and Tans, P. P.: NOAA Greenhouse Gas Reference from Atmospheric Carbon Dioxide Dry Air Mole Fractions from the NOAA ESRL Carbon Cycle Cooperative Global Air Sampling Network, Data Path: ftp://aftp.cmdl.noaa.gov/data/trace_gases/co2/flask/surface/ (last access: 1 September 2017), 2015.
- Eveleth, R., Cassar, N., Doney, S. C., Munro, D. R., and Sweeney, C.: Biological and physical controls on O_2/Ar , Ar and pCO_2 variability at the Western Antarctic Peninsula and in the Drake Passage, *Deep-Sea Res. Pt. II*, 139, 77–88, 2017.
- Fay, A. R. and McKinley, G. A.: Global trends in surface ocean pCO_2 from in situ data, *Global Biogeochem. Cy.*, 27, 541–557, 2013.
- Fay, A. R. and McKinley, G. A.: Global open-ocean biomes: mean and temporal variability, *Earth Syst. Sci. Data*, 6, 273–284, <https://doi.org/10.5194/essd-6-273-2014>, 2014.
- Fay, A. R., McKinley, G. A., and Lovenduski, N. S.: Southern Ocean carbon trends: Sensitivity to methods, *Geophys. Res. Lett.*, 41, 6833–6840, 2014.
- Freeman, N. M. and Lovenduski, N. S.: Mapping the Antarctic Polar Front: weekly realizations from 2002 to 2014, *Earth Syst. Sci. Data*, 8, 191–198, <https://doi.org/10.5194/essd-8-191-2016>, 2016.
- Freeman, N. M., Lovenduski, N. S., and Gent, P. R.: Temporal variability in the Antarctic Polar Front (2001–2014), *J. Geophys. Res.-Oceans*, 121, 7263–7276, <https://doi.org/10.1002/2016JC012145>, 2016.
- Frölicher, T. L., Sarmiento, J. L., Paynter, D. J., Dunne, J. P., Krasting, J. P., and Winton, M.: Dominance of the Southern Ocean in anthropogenic carbon and heat uptake in CMIP5 models, *J. Climate*, 28, 862–886, 2015.
- Gregor, L., Kok, S., and Monteiro, P. M. S.: Interannual drivers of the seasonal cycle of CO_2 in the Southern Ocean, *Biogeosciences*, 15, 2361–2378, <https://doi.org/10.5194/bg-15-2361-2018>, 2018.
- Gruber, N., Gloor, M., Mikaloff Fletcher, S. E., Doney, S. C., Dutkiewicz, S., Follows, M. J., Gerber, M., Jacobson, A. R., Joos, F., Lindsay, K., Menemenlis, D., Mouchet, A., Müller, S. A., Sarmiento, J. L., and Takahashi, T.: Oceanic sources, sinks, and transport of atmospheric CO_2 , *Global Biogeochem. Cy.*, 23, GB1005, <https://doi.org/10.1029/2008GB003349>, 2009.
- Hoppema, M., Velo, A., van Heuven, S., Tanhua, T., Key, R. M., Lin, X., Bakker, D. C. E., Perez, F. F., Ríos, A. F., Lo Monaco, C., Sabine, C. L., Álvarez, M., and Bellerby, R. G. J.: Consistency of cruise data of the CARINA database in the Atlantic sector of the Southern Ocean, *Earth Syst. Sci. Data*, 1, 63–75, <https://doi.org/10.5194/essd-1-63-2009>, 2009.
- Johnson, K. S., Jannasch, H. W., Coletti, L. J., Elrod, V. A., Martz, T. R., Takeshita, Y., Carlson, R. J., and Connery, J. G.: Deep-Sea DuraFET: A pressure tolerant pH sensor designed for global sensor networks, *Anal. Chem.*, 88, 3249–3256, 2016.
- Johnson, K. S., Plant, J. N., Coletti, L. J., Jannasch, H. W., Sakamoto, C. M., Riser, S. C., and Talley, L. D.: Biogeochemical sensor performance in the SOCCOM profiling float array, *J. Geophys. Res.-Oceans*, 122, 6416–6436, <https://doi.org/10.1002/2017JC012838>, 2017.
- Johnson, K. S., Riser, S. C., Boss, E. S., Talley, L. D., Sarmiento, J. L., Swift, D. D., Plant, J. N., Maurer, T. L., Key, R. M., Williams, N. L., Wanninkhof, R. H., Dickson, A. G., Feely, R. A., and Russell, J. L.: SOCCOM float data – Snapshot 2018-03-06, in: *Southern Ocean Carbon and Climate Observations and Modeling (SOCCOM) Float Data Archive*, UC San Diego Library Digital Collections, <https://doi.org/10.6075/JOPG1PX7>, 2018.
- Landschützer, P., Gruber, N., Bakker, D. C. E., and Schuster, U.: Recent variability of the global ocean carbon sink, *Global Biogeochem. Cy.*, 28, 927–949, <https://doi.org/10.1002/2014GB004853>, 2014a.
- Landschützer, P., Gruber, N., Bakker, D. C. E., and Schuster, U.: An observation-based global monthly gridded sea surface pCO_2 product from 1998 through 2011 and its monthly climatology, available on: http://cdiac.ornl.gov/oceans/SPCO2_1998_2011_ETH_SOM_FFN.html (last access: 22 November 2017), 2014b.
- Landschützer, P., Gruber, N., Haumann, F., Rödenbeck, C., Bakker, D., van Heuven, S., Hoppema, M., Metzl, N., Sweeney, C., Takahashi, T., Tilbrook, B., and Wanninkhof, R.: The reinvigoration of the Southern Ocean carbon sink, *Science*, 349, 1221–1224, 2015a.
- Landschützer, P., Gruber, N., and Bakker, D. C. E.: A 30 years observation-based global monthly gridded sea surface pCO_2 product from 1982 through 2011, http://cdiac.ornl.gov/ftp/oceans/SPCO2_1982_2011_ETH_SOM_FFN, Carbon Dioxide Information Analysis Center, Oak Ridge National Laboratory, US Department of Energy, Oak Ridge, Tennessee, https://doi.org/10.3334/CDIAC/OTG.SPACO2_1982_2011_ETH_SOMFFN, 2015b.
- Landschützer, P., Gruber, N., and Bakker, D. C. E.: Decadal variations and trends of the global ocean carbon sink, *Global Biogeochem. Cy.*, 30, 1396–1417, <https://doi.org/10.1002/2015GB005359>, 2016.
- Landschützer, P., Gruber, N., and Bakker, D. C. E.: An updated observation-based global monthly gridded sea surface pCO_2 and air-sea CO_2 flux product from 1982 through 2015 and its monthly climatology (NCEI Accession 0160558). Version 2.2. NOAA National Centers for Environmental Information.

- Dataset. [2017-07-11]: available at: https://www.nodc.noaa.gov/ocads/oceans/SPCO2_1982_2015_ETH_SOM_FFNN.html, 2017.
- Le Quéré, C., Rödenbeck, C., Buitenhuis, E. T., Conway, T. J., Langenfelds, R., Gomez, A., Labuschagne, C., Ramonet, M., Nakazawa, T., Metzl, N., Gillett, N., and Heimann, M.: Saturation of the Southern Ocean CO₂ sink due to recent climate change, *Science*, 316, 1735–1738, <https://doi.org/10.1126/science.1136188>, 2007.
- Le Quéré, C., Andrew, R. M., Canadell, J. G., Sitch, S., Korsbakken, J. I., Peters, G. P., Manning, A. C., Boden, T. A., Tans, P. P., Houghton, R. A., Keeling, R. F., Alin, S., Andrews, O. D., Anthoni, P., Barbero, L., Bopp, L., Chevallier, F., Chini, L. P., Ciais, P., Currie, K., Delire, C., Doney, S. C., Friedlingstein, P., Gkritzalis, T., Harris, I., Hauck, J., Haverd, V., Hoppema, M., Klein Goldewijk, K., Jain, A. K., Kato, E., Körtzinger, A., Landschützer, P., Lefèvre, N., Lenton, A., Lienert, S., Lombardozi, D., Melton, J. R., Metzl, N., Millero, F., Monteiro, P. M. S., Munro, D. R., Nabel, J. E. M. S., Nakaoka, S.-I., O'Brien, K., Olsen, A., Omar, A. M., Ono, T., Pierrot, D., Poulter, B., Rödenbeck, C., Salisbury, J., Schuster, U., Schwinger, J., Séférian, R., Skjelvan, I., Stocker, B. D., Sutton, A. J., Takahashi, T., Tian, H., Tilbrook, B., van der Laan-Luijkx, I. T., van der Werf, G. R., Viovy, N., Walker, A. P., Wiltshire, A. J., and Zaehle, S.: Global Carbon Budget 2016, *Earth Syst. Sci. Data*, 8, 605–649, <https://doi.org/10.5194/essd-8-605-2016>, 2016.
- Le Quéré, C., Andrew, R. M., Friedlingstein, P., Sitch, S., Pongratz, J., Manning, A. C., Korsbakken, J. I., Peters, G. P., Canadell, J. G., Jackson, R. B., Boden, T. A., Tans, P. P., Andrews, O. D., Arora, V. K., Bakker, D. C. E., Barbero, L., Becker, M., Betts, R. A., Bopp, L., Chevallier, F., Chini, L. P., Ciais, P., Cosca, C. E., Cross, J., Currie, K., Gasser, T., Harris, I., Hauck, J., Haverd, V., Houghton, R. A., Hunt, C. W., Hurtt, G., Ilyina, T., Jain, A. K., Kato, E., Kautz, M., Keeling, R. F., Klein Goldewijk, K., Körtzinger, A., Landschützer, P., Lefèvre, N., Lenton, A., Lienert, S., Lima, I., Lombardozi, D., Metzl, N., Millero, F., Monteiro, P. M. S., Munro, D. R., Nabel, J. E. M. S., Nakaoka, S.-I., Nojiri, Y., Padin, X. A., Peregon, A., Pfeil, B., Pierrot, D., Poulter, B., Rehder, G., Reimer, J., Rödenbeck, C., Schwinger, J., Séférian, R., Skjelvan, I., Stocker, B. D., Tian, H., Tilbrook, B., Tubiello, F. N., van der Laan-Luijkx, I. T., van der Werf, G. R., van Heuven, S., Viovy, N., Vuichard, N., Walker, A. P., Watson, A. J., Wiltshire, A. J., Zaehle, S., and Zhu, D.: Global Carbon Budget 2017, *Earth Syst. Sci. Data*, 10, 405–448, <https://doi.org/10.5194/essd-10-405-2018>, 2018.
- Lo Monaco, C., Metzl, N., Poisson, A., Brunet, C., and Schauer, B.: Anthropogenic CO₂ in the Southern Ocean: Distribution and inventory at the Indian-Atlantic boundary (World Ocean Circulation Experiment line I6), *J. Geophys. Res.-Oceans*, 110, C06010, <https://doi.org/10.1029/2004JC002643>, 2005.
- Lo Monaco, C., Álvarez, M., Key, R. M., Lin, X., Tanhua, T., Tilbrook, B., Bakker, D. C. E., van Heuven, S., Hoppema, M., Metzl, N., Ríos, A. F., Sabine, C. L., and Velo, A.: Assessing the internal consistency of the CARINA database in the Indian sector of the Southern Ocean, *Earth Syst. Sci. Data*, 2, 51–70, <https://doi.org/10.5194/essd-2-51-2010>, 2010.
- Lovenduski, N. S., Gruber, N., and Doney, S. C.: Toward a mechanistic understanding of the decadal trends in the Southern Ocean carbon sink, *Global Biogeochem. Cy.*, 22, GB3016, <https://doi.org/10.1029/2007GB003139>, 2008.
- Lovenduski, N. S., Fay, A. R., and McKinley, G. A.: Observing multidecadal trends in Southern Ocean CO₂ uptake: What can we learn from an ocean model?, *Global Biogeochem. Cy.*, 29, 416–426, <https://doi.org/10.1002/2014GB004933>, 2015.
- Majkut, J. D., Carter, B. R., Frölicher, T. L., Dufour, C. O., Rodgers, K. B., and Sarmiento, J. L.: An observing system simulation for Southern Ocean carbon dioxide uptake, *Phil. Trans. R. Soc. A*, 372, 2019, 20130046, 2014.
- McKinley, G. A., Fay, A. R., Lovenduski, N. S., and Pilcher, D. J.: Natural variability and anthropogenic trends in the ocean carbon sink, *Annu. Rev. Mar. Sci.*, 9, 125–150, 2017.
- Metzl, N.: Decadal increase of oceanic carbon dioxide in Southern Indian Ocean surface waters (1991–2007), *Deep-Sea Res. Pt. II*, 56, 607–619, 2009.
- Metzl, N., Tilbrook, B., and Poisson, A.: The annual fCO₂ cycle and the air-sea CO₂ flux in the sub-Antarctic Ocean, *Tellus B*, 51, 849–861, 1999.
- Munro, D. R., Lovenduski, N. S., Takahashi, T., Stephens, B. B., Newberger, T., and Sweeney, C.: Recent evidence for a strengthening CO₂ sink in the Southern Ocean from carbonate system measurements in the Drake Passage (2002–2015), *Geophys. Res. Lett.*, 42, 7623–7630, <https://doi.org/10.1002/2015GL065194>, 2015a.
- Munro, D. R., Lovenduski, N. S., Stephens, B. B., Newberger, T., Arrigo, K. R., Takahashi, T., Quay, P. D., Sprintall, J., Freeman, N. M., and Sweeney, C.: Estimates of net community production in the Southern Ocean determined from time-series observations (2002–2011) of nutrients, dissolved inorganic carbon, and surface ocean pCO₂ in Drake Passage, *Deep-Sea Res. Pt. II*, 114, 49–63, <https://doi.org/10.1016/j.dsr2.2014.12.014>, 2015b.
- Olsen, A., Metzl, N., Bakker, D., and O'Brien, K.: SOCAT QC cookbook for SOCAT participants; available at: https://www.socat.info/wp-content/uploads/2017/04/2015_SOCAT_QC_Cookbook_v3.pdf (last access: 1 November 2017), 2013.
- Pfeil, B., Olsen, A., Bakker, D. C. E., Hankin, S., Koyuk, H., Kozyr, A., Malczyk, J., Manke, A., Metzl, N., Sabine, C. L., Akl, J., Alin, S. R., Bates, N., Bellerby, R. G. J., Borges, A., Boutin, J., Brown, P. J., Cai, W.-J., Chavez, F. P., Chen, A., Cosca, C., Fassbender, A. J., Feely, R. A., González-Dávila, M., Goyet, C., Hales, B., Hardman-Mountford, N., Heinze, C., Hood, M., Hoppema, M., Hunt, C. W., Hydes, D., Ishii, M., Johannessen, T., Jones, S. D., Key, R. M., Körtzinger, A., Landschützer, P., Lauvset, S. K., Lefèvre, N., Lenton, A., Lourantou, A., Merlivat, L., Midorikawa, T., Mintrop, L., Miyazaki, C., Murata, A., Nakadate, A., Nakano, Y., Nakaoka, S., Nojiri, Y., Omar, A. M., Padin, X. A., Park, G.-H., Paterson, K., Perez, F. F., Pierrot, D., Poisson, A., Ríos, A. F., Santana-Casiano, J. M., Salisbury, J., Sarma, V. V. S. S., Schlitzer, R., Schneider, B., Schuster, U., Sieger, R., Skjelvan, I., Steinhoff, T., Suzuki, T., Takahashi, T., Tedesco, K., Telszewski, M., Thomas, H., Tilbrook, B., Tjiputra, J., Vandemark, D., Veness, T., Wanninkhof, R., Watson, A. J., Weiss, R., Wong, C. S., and Yoshikawa-Inoue, H.: A uniform, quality controlled Surface Ocean CO₂ Atlas (SOCAT), *Earth Syst. Sci. Data*, 5, 125–143, <https://doi.org/10.5194/essd-5-125-2013>, 2013.
- Rödenbeck, C., Bakker, D. C. E., Gruber, N., Iida, Y., Jacobson, A. R., Jones, S., Landschützer, P., Metzl, N., Nakaoka,

- S., Olsen, A., Park, G.-H., Peylin, P., Rodgers, K. B., Sasse, T. P., Schuster, U., Shutler, J. D., Valsala, V., Wanninkhof, R., and Zeng, J.: Data-based estimates of the ocean carbon sink variability – first results of the Surface Ocean $p\text{CO}_2$ Mapping intercomparison (SOCOM), *Biogeosciences*, 12, 7251–7278, <https://doi.org/10.5194/bg-12-7251-2015>, 2015.
- Sabine, C. L., Hankin, S., Koyuk, H., Bakker, D. C. E., Pfeil, B., Olsen, A., Metzl, N., Kozyr, A., Fassbender, A., Manke, A., Malczyk, J., Akl, J., Alin, S. R., Bellerby, R. G. J., Borges, A., Boutin, J., Brown, P. J., Cai, W.-J., Chavez, F. P., Chen, A., Cosca, C., Feely, R. A., González-Dávila, M., Goyet, C., Hardman-Mountford, N., Heinze, C., Hoppema, M., Hunt, C. W., Hydes, D., Ishii, M., Johannessen, T., Key, R. M., Körtzinger, A., Landschützer, P., Lauvset, S. K., Lefèvre, N., Lenton, A., Lourantou, A., Merlivat, L., Midorikawa, T., Mintrop, L., Miyazaki, C., Murata, A., Nakadate, A., Nakano, Y., Nakaoka, S., Nojiri, Y., Omar, A. M., Padin, X. A., Park, G.-H., Paterson, K., Perez, F. F., Pierrot, D., Poisson, A., Ríos, A. F., Salisbury, J., Santana-Casiano, J. M., Sarma, V. V. S. S., Schlitzer, R., Schneider, B., Schuster, U., Sieger, R., Skjelvan, I., Steinhoff, T., Suzuki, T., Takahashi, T., Tedesco, K., Telszewski, M., Thomas, H., Tilbrook, B., Vandemark, D., Veness, T., Watson, A. J., Weiss, R., Wong, C. S., and Yoshikawa-Inoue, H.: Surface Ocean CO_2 Atlas (SOCAT) gridded data products, *Earth Syst. Sci. Data*, 5, 145–153, <https://doi.org/10.5194/essd-5-145-2013>, 2013.
- Shadwick, E. H., Trull, T. W., Tilbrook, B., Sutton, A. J., Schulz, E., and Sabine, C. L.: Seasonality of biological and physical controls on surface ocean CO_2 from hourly observations at the Southern Ocean Time Series site south of Australia, *Global Biogeochem. Cy.*, 29, 223–238, 2015.
- Sprintall, J., Chereskin, T. K., and Sweeney, C.: High-resolution underway upper ocean and surface atmospheric observations in Drake Passage: Synergistic measurements for climate science., *Oceanography*, 25, 70–81, 2012.
- Takahashi, T., Sutherland, S. C., Sweeney, C., Poisson, A., Metzl, N., Tilbrook, B., Bates, N., Wanninkhof, R., Feely, R. F., Sabine, C., Olafsson, J., and Nojiri, Y.: Global sea-air CO_2 flux based on climatological surface ocean $p\text{CO}_2$ and seasonal biological and temperature effects, *Deep-Sea Res. Pt. II*, 49, 1601–1622, 2002.
- Takahashi, T., Sutherland, S., Wanninkhof, R., Sweeney, C., Feely, R., Chipman, D., Hales, B., Friederich, G., Chavez, F., Sabine, C., Watson, A., Bakker, D., Schuster, U., Metzl, N., Yoshikawa-Inoue, H., Ishii, M., Midorikawa, T., Nojiri, Y., Körtzinger, A., Steinhoff, T., Hoppema, M., Olafson, J., Arnarson, T., Tilbrook, B., Johannessen, T., Olsen, A., Bellerby, R., Wong, C., Delille, B., Bates, N., and de Baar, H.: Climatological mean and decadal change in surface ocean $p\text{CO}_2$, and net sea-air CO_2 flux over the global oceans, *Deep-Sea Res. Pt. II*, 56, 554–577, 2009.
- Takahashi, T., Sweeney, C., Hales, B., Chipman, D. W., Newberger, T., Goddard, J. G., Iannuzzi, R. A., and Sutherland, S. C.: The changing carbon cycle in the Southern Ocean, *Oceanography*, 25, 26–37, 2012.
- Takahashi, T., Sutherland, S. C., Chipman, D. W., Goddard, J. G., Ho, C., Newberger, T., Sweeney, C., and Munro, D. R.: Climatological Distributions of pH, $p\text{CO}_2$, Total CO_2 , Alkalinity, and CaCO_3 Saturation in the Global Surface Ocean, and Temporal Changes at Selected Locations, *Mar. Chem.*, 164, 95–125, <https://doi.org/10.7916/D8G73D37>, 2014.
- Takahashi, T., Sutherland, S. C., and Kozyr, A.: Global Ocean Surface Water Partial Pressure of CO_2 Database: Measurements Performed During 1957–2017 (LDEO Database Version 2017) (NCEI Accession 0160492). Version 6.6. NOAA National Centers for Environmental Information, Dataset, [https://doi.org/10.3334/CDIAC/OTG.NDP088\(V2015\)](https://doi.org/10.3334/CDIAC/OTG.NDP088(V2015)) (last access: 2 April 2018), 2017.
- van Heuven, S. M., Hoppema, M., Huhn, O., Slagter, H. A., and de Baar, H. J.: Direct observation of increasing CO_2 in the Weddell Gyre along the Prime Meridian during 1973–2008, *Deep-Sea Res. Pt. II*, 58, 2613–2635, 2011.
- Williams, N. L., Juranek, L. W., Johnson, K. S., Feely, R. A., Riser, S. C., Talley, L. D., Russell, J. L., Sarmiento, J. L., and Wanninkhof, R.: Empirical algorithms to estimate water column pH in the Southern Ocean, *Geophys. Res. Lett.*, 43, 3415–3422, 2016.
- Williams, N. L., Juranek, L. W., Feely, R. A., Johnson, K. S., Sarmiento, J. L., Talley, L. D., and Riser, S. C.: Calculating surface ocean $p\text{CO}_2$ from biogeochemical Argo floats equipped with pH: an uncertainty analysis, *Global Biogeochem. Cy.*, 31, 591–604, 2017.
- Xue, L., Gao, L., Cai, W. J., Yu, W., and Wei, M.: Response of sea surface fugacity of CO_2 to the SAM shift south of Tasmania: Regional differences, *Geophys. Res. Lett.*, 42, 3973–3979, 2015.